# CMB Peaks and Early-Time Constraints on the MMA–DMF Model (Planck, ACT and Simons)

Paulo Adriano

November 23, 2025

**Abstract**

This paper presents an extensive and technical assessment of early-time observational constraints on the cosmological model Modified Matter Acceleration–Dark Matter Free (MMA–DMF). In response to the persistent tensions that challenge the standard ΛCDM paradigm — notably the $5\sigma$ Hubble tension and the continued null results of direct detection experiments for Cold Dark Matter (CDM) particles — the MMA–DMF model proposes a unified cosmological history that relies exclusively on baryonic matter and a scalar-mediated modification of gravity.

The scope of this document is strictly focused on the "Primordial Universe" sector ($z > 1000$), where we test the model against high-precision data from the Planck 2018 release (temperature and polarization), the Atacama Cosmology Telescope (ACT) DR6, and Baryon Acoustic Oscillation (BAO) measurements. We detail the theoretical infrastructure of the model, which introduces a transient radiation "EARLY Bump" (parametrized by $f_{\text{peak}} = 0.36$ and $p = 3$) and an effective decaying X-component designed to mimic the gravitational potential wells of CDM prior to recombination.

Crucially, the analysis shows that the model, under strict "No-Slip" conditions ($\Phi = \Psi$) and General-Relativistic lensing kernels ($\Sigma = 1$) during the CMB epoch, reproduces the acoustic scale $\theta_*$ with 0.01% precision relative to Planck observations. Numerical results indicate that the model naturally accommodates a local Hubble constant of $H_0 \simeq 72\,\text{km}\,\text{s}^{-1}\,\text{Mpc}^{-1}$ through a geometric modification of the sound horizon ($r_s \simeq 137\,\text{Mpc}$).

We conclude, invoking the principle of parsimony, that the MMA–DMF framework provides a phenomenologically viable early-time alternative that fits current data without an explicit CDM component, with the Hubble constant emerging geometrically.

## Contents

# 1 Introduction: Cosmological Context and the MMA–DMF Paradigm

## 1.1 The State of Precision Cosmology and Emerging Tensions

The standard cosmological model, known as ΛCDM, represents the current peak of our understanding of the large-scale evolution of the Universe. It successfully reconciles a wide range of observational data, from the recession of distant galaxies and the abundances of light elements synthesized in the Big Bang, to the exquisite temperature anisotropies imprinted in the Cosmic Microwave Background (CMB). This framework rests on the existence of two dominant yet invisible components: Dark Energy (Λ), responsible for late-time accelerated expansion, and Cold Dark Matter (CDM), a non-baryonic, collisionless fluid required to facilitate gravitational collapse of structures and stabilize acoustic oscillations in the primordial plasma.

Despite its profound phenomenological success, ΛCDM now faces both theoretical dissatisfaction and observational discord. On the theoretical side, the nature of the dark sector remains elusive; after decades of sensitive direct-detection experiments, no particle candidate for Dark

Matter has been observed. On the observational side, precision cosmology has entered an era of "tensions". The most statistically significant of these is the Hubble tension — a roughly 9% discrepancy between the cosmic expansion rate ($H_0$) inferred from primordial probes such as the CMB (assuming ΛCDM physics) and the rate measured directly in the local Universe via Cepheid variables and Type Ia supernovae. Planck 2018 data suggest $H_0 \approx 67.4\,\mathrm{km\,s^{-1}\,Mpc^{-1}}$, while the SH0ES collaboration reports $H_0 \approx 73.0\,\mathrm{km\,s^{-1}\,Mpc^{-1}}$, a $5\sigma$ discrepancy.

### 1.2 The MMA–DMF Proposal and the Cyclic Hypothesis

The Modified Matter Acceleration–Dark Matter Free (MMA–DMF) model proposes a radical alternative: a Universe devoid of particulate Dark Matter, where the phenomenology of "missing mass" is an emergent property of modified gravitational interaction and a unified expansion history, discussed in this report, is built on a distinct cyclic premise in which the Universe does not emerge from a conventional singularity, but from a turnaround or bounce process.

In this cyclic hypothesis, the previous Universe collapses into a single primordial supermassive black hole (MBH) containing virtually all the mass of the previous cycle. Above some as-yet unknown generalization of the Tolman–Oppenheimer–Volkoff (TOV) limit, this core collapses and triggers an outflow analogous to a "white hole" — our Big Bang. During a subsequent superluminal inflationary phase, information from the previous cycle is erased, but the scalar field reaches maximal amplitude and range. Consequently, the "fifth force" is already active before recombination, influencing primordial dynamics in ways that late-time modified gravity models do not anticipate.

This theoretical setup demands distinct but coupled "EARLY" (early-time) and "LATE" (late-time) sectors, both governed by the evolution of the same scalar field. The central hypothesis for the primordial era is that the effects of Dark Matter on the CMB — specifically the depth of gravitational potential wells and the expansion rate — can be mimicked by a transient modification of the background energy density and a scalar field that strictly obeys GR constraints during recombination.

### 1.3 Scope and Objectives of the Report

This document serves as a rigorous technical validation of the early-time sector of the MMA–DMF model. It does not address late-time galactic rotation curves or cluster dynamics in depth, except where these intersect linear structure growth. The primary objectives are:

- To detail the mathematical formulation of the unified Hubble function $E(a)$ and the transient X-component.
- To present an explicit Data & Likelihoods section describing the Planck, ACT, and BAO inputs.
- To describe in detail the numerical results of the $r_s$-free BAO method.
- To provide comprehensive parameter tables with uncertainties and $\chi^2$ statistics.
- To moderate the assertive tone, providing an objective evaluation of the model's viability against Planck 2018 primary anisotropies (TT, TE, EE) and the acoustic scale $\theta_*$.
- To verify the consistency of the linear matter power spectrum $P(k)$ with standard ΛCDM predictions.

## 2 Theoretical Foundation: The Unified Background Sector

The core of the MMA–DMF early-time solution is a restructuring of the background expansion history. In the standard model, the expansion rate $H(z)$ is determined by the sum of radiation, baryonic matter, cold dark matter, and dark energy. MMA–DMF removes the CDM component entirely ($\Omega_c = 0$) and compensates this deficit via a unified-fluid description that introduces transient energy-density components.

## 2.1 The Unified Hubble Function $E(a)$

The evolution of the Hubble parameter, normalized as $E(a) \equiv H(a)/H_0$, is governed by a modified Friedmann equation. This equation must smoothly connect a radiation-dominated era (modified to resolve the Hubble tension) to a late-time vacuum-dominated era (modified to replace Dark Matter). The explicit form used in MMA–DMF is

$$E^2(a) = \Omega_r a^{-4} + \left[\Omega_b + \Omega_X^{\text{early}} \chi(a)\right] a^{-3} + \Omega_{\Lambda,0}^{\text{eff}} . \tag{1}$$

Here $\Omega_{\Lambda,0}^{\text{eff}}$ is fixed by flatness so that $E(1) = 1$.

This formulation introduces two critical phenomenological components: the radiation "EARLY Bump" and the transient X-component.

### 2.1.1 The Radiation EARLY Bump ($f_{\text{peak}}$)

To resolve the Hubble tension geometrically, the comoving sound horizon at the drag epoch $r_s$ must be reduced. The sound horizon is defined as

$$r_s(z_d) = \int_{z_d}^{\infty} \frac{c_s(z)}{H(z)} \, \mathrm{d}z . \tag{2}$$

Since $H(z)$ appears in the denominator, increasing the expansion rate during the pre-recombination era reduces $r_s$. MMA–DMF achieves this via a localized injection of energy density modeled by the shape function $S_{\text{eq}}(a)$:

$$S_{\text{eq}}(a) = \frac{(a/a_{\text{eq}})^p}{1 + (a/a_{\text{eq}})^p} . \tag{3}$$

The parameters are:

- Amplitude $f_{\text{peak}}$: defines the maximum fractional increase in the radiation density. The reference value for the present Planck-tuned run is $f_{\text{peak}} = 0.36$ (0.18 in earlier iterations).
- Slope $p$: controls the sharpness of the transition. The model fixes $p = 3$, producing a smooth but distinct rise and fall in the energy density.
- Location $a_{\text{eq}}$: the injection is centered near the standard matter–radiation equality epoch, $z_{\text{eq}} \approx 3400$.

Physically, this bump represents a transient phase in the evolution of the unified field, possibly linked to the decay of the primordial black hole remnant or a resonance in the scalar sector. Crucially, as $a \to 0$, $S_{\text{eq}}(a) \to 0$ rapidly (as $a^3$). This ensures that during Big Bang Nucleosynthesis (BBN, $z \sim 10^9$), the expansion rate is standard, thereby preserving the delicate light-element abundances (He-4, deuterium). The model enforces a stringent bound that the extra energy density during BBN is negligible ($\Delta N_{\text{eff}} \approx 0$ during BBN).

### 2.1.2 The Transient X-Component ($\Omega_X$)

In a purely baryonic Universe ($\Omega_b \approx 0.05$), the epoch of matter–radiation equality would occur much later than in $\Lambda$CDM ($\Omega_m \approx 0.30$). This delay would fundamentally change the forcing of acoustic oscillators in the CMB, shifting both positions and amplitudes of the peaks in unacceptable ways. To avoid this, MMA–DMF introduces an effective matter-like component $\Omega_X$

that mimics CDM's gravitational inertia during the radiation era but decays before the Universe becomes transparent.

This component is governed by a switching function $\chi(a)$:

$$\Omega_X^{\text{early}}(a) = \Omega_{X,0}\, a^{-3}\, \chi(a)\,, \tag{4}$$

where $\chi(a)$ is a smooth step function transitioning from 1 (active) to 0 (inactive) around a redshift $z_{\text{switch}} \approx 850$, with slope parameter $m_{\text{switch}} = 6$. We can distinguish two regimes:

- Early regime ($z > 1000$): $\chi(a) \approx 1$. The Universe expands as if it contained CDM. Gravitational potentials decay at the standard rate, correctly driving the acoustic oscillations.
- Late regime ($z < 800$): $\chi(a) \approx 0$. The X-component disappears (decays into radiation or scalar-field energy), leaving a Universe containing only baryons and dark energy.

### 2.2 Thermodynamics and Energy Exchange

Introducing transient components requires a careful thermodynamic treatment to ensure energy conservation or at least a consistent exchange. The model postulates an interaction between the X-component and the radiation bath, described by continuity equations

$$\frac{\mathrm{d}\rho_X}{\mathrm{d}\ln a} + 3\rho_X = -\frac{\Gamma}{H}\,\rho_X\,, \tag{5}$$

$$\frac{\mathrm{d}\rho_\gamma}{\mathrm{d}\ln a} + 4\rho_\gamma = +\frac{\Gamma}{H}\,\rho_X\,. \tag{6}$$

Here $\Gamma$ is the decay rate. This interaction guarantees that as the X-component disappears, its energy is transferred to the radiation sector (or to the scalar reservoir), thereby avoiding any violation of the first law of thermodynamics. The rate $\Gamma$ is tuned such that the transition occurs after the acoustic pattern is set, but before late-time structure growth begins.

## 3 Scalar-Sector Microphysics: Gravity and Baryogenesis

While the modified background deals with the expansion history, structure formation in a baryon-only Universe requires a modification to gravity. In MMA–DMF, this is mediated by a scalar field $\varphi$.

### 3.1 Action and Field Equations

The theory is defined by a scalar–tensor action in which metric coupling is modified by a conformal function $A(\varphi)$:

$$S = \int \mathrm{d}^4x\,\sqrt{-g}\,\mathcal{L}\big[g_{\mu\nu}, \varphi, \text{matter}\big]\,. \tag{7}$$

Matter fields (baryons) follow geodesics of the conformally related metric

$$\tilde{g}_{\mu\nu} = A^2(\varphi)\, g_{\mu\nu}\,. \tag{8}$$

This results in a fifth force acting on baryons but not on photons (which are conformally invariant at the classical level). The scalar field obeys a Klein–Gordon equation with a matter-dependent source term

$$(\nabla^2 - m_{\text{eff}}^2)\,\varphi = \frac{\beta(\varphi)}{M_{\text{Pl}}}\,\rho_b\,, \tag{9}$$

where $\beta(\varphi)$ parameterizes the coupling strength. The field mass $m_{\text{eff}}$ determines the range $\lambda = m_{\text{eff}}^{-1}$. Crucially, the mass is environment dependent, enabling screening mechanisms such as the chameleon or curvature-coupled screening, which are essential to hide the fifth force in dense regions.

### 3.2 The No-Slip Guard ($\Phi = \Psi$)

A critical innovation of the MMA–DMF early-time pipeline is the strict separation of background dynamics from perturbation potentials during recombination. In many modified gravity theories, the relation between the Newtonian potential (time–time metric perturbation) and the curvature potential (space–space perturbation) is altered, quantified by the slip parameter $\eta = \Phi/\Psi \neq 1$. CMB data impose tight constraints on $\eta$ via the Integrated Sachs–Wolfe (ISW) effect.

MMA–DMF enforces a strict No-Slip guard for the high-redshift Universe. The operational rule for the Boltzmann solver is

$$z > 100 \;\Rightarrow\; \eta(a,k) \equiv \frac{\Phi}{\Psi} = 1\,, \tag{10}$$

$$\mu(a,k) \equiv \frac{G_{\rm eff}}{G} = 1 \qquad \text{(linear regime)}\,. \tag{11}$$

This implies that while the background expansion $H(a)$ is modified (affecting timing and distances), the physics of acoustic oscillators remains governed by standard GR. Photons and baryons oscillate in potential wells that evolve according to GR. The scalar field is effectively dormant in its perturbative capacity during this epoch, activating its role as a force mediator only at late times ($z < 100$) to boost structure formation. This No-Slip condition is essential to preserving the phase coherence of CMB peaks.

### 3.3 Spontaneous Baryogenesis

In a model without Dark Matter, the baryon density $\Omega_b$ becomes the only matter source. A fundamental question then arises: where does this specific amount of matter come from? The MMA–DMF framework integrates the generation of baryon asymmetry directly into the scalar sector via Spontaneous Baryogenesis.

The model postulates a derivative coupling between the scalar field and the baryon-minus-lepton current $J^\mu_{B-L}$:

$$\mathcal{L}_{\rm baryo} = \frac{\partial_\mu \varphi}{M_B}\, J^\mu_{B-L}\,. \tag{12}$$

This interaction generates an effective chemical potential

$$\mu_{B-L} = \frac{\dot\varphi}{M_B} \tag{13}$$

for baryons whenever the field evolves ($\dot\varphi \neq 0$). This violates CPT and biases the production of matter over antimatter. The final baryon asymmetry $\eta_B$ is frozen when interactions decouple at a temperature $T_f$. The predicted asymmetry is

$$\eta_B \simeq \frac{15}{4\pi^2}\,\frac{g_B}{g_*}\,\frac{\dot\varphi}{M_B T_f}\,. \tag{14}$$

By fixing the freeze-out temperature near the electroweak scale ($T_f \approx 140\,\mathrm{GeV}$) and tuning the scale $M_B$, the model naturally reproduces the observed baryon-to-photon ratio $\eta_B^{\rm obs} \simeq 6\times10^{-10}$. To avoid spoiling BBN, the scalar-field energy density during baryogenesis is constrained to $f_\varphi = \rho_\varphi/\rho_{\rm rad} \leq 10^{-3}$. This implies a negligible contribution to the effective number of neutrino species ($\Delta N_{\rm eff} \leq 0.0075$), well within Planck bounds.

## 4 Analysis Methodology: The $r_s$-free Pipeline and Boltzmann Implementation

To validate this theoretical framework, we employ a testing pipeline that avoids the biases inherent to standard cosmological analyses, which frequently assume a fixed ΛCDM sound horizon.

### 4.1 Modified Boltzmann Solver

We use a custom-modified version of the `CLASS` Boltzmann code. The main modifications are:

- **Background module:** the standard Friedmann solver is replaced by the unified function $E(a)$ in Eq. (1). This forces the code to integrate the unified history, including the EARLY Bump and the transient X-component, directly.
- **Perturbation module:** the equations for the density contrast $\delta$ and velocity divergence $\theta$ are modified to exclude stable CDM as a species. Instead, the X-component is treated as a decaying fluid.
- **Lensing kernel:** the lensing kernel is forced to its GR form ($\Sigma = 1$). The lensing potential is computed from the matter distribution using the standard Poisson equation, even though the matter power spectrum $P(k)$ itself grows under the influence of the scalar force in the non-linear regime (treated by effective transfer functions).

### 4.2 The $r_s$-free BAO Analysis Protocol

Standard BAO analyses usually quote a distance ratio $D_V/r_s^{\mathrm{fid}}$. If the true Universe has a different $r_s$ (as in MMA–DMF, with $r_s \approx 137\,\mathrm{Mpc}$ vs $147\,\mathrm{Mpc}$), using a fixed fiducial $r_s$ biases the result. MMA–DMF employs an $r_s$-free pipeline to analyse galaxy clustering data:

1. **Grid alignment:** theoretical power spectra $P_{\mathrm{th}}(k)$ are resampled to match the exact $k$-bins of the survey covariance matrix via a linear operator $S$. The rule is to align the vector, never re-bin the covariance matrix $C$.
2. **Broadband removal:** a smooth "no-wiggle" component $P_{\mathrm{nw}}(k)$ is fitted and subtracted from both data and model to isolate the oscillatory (acoustic) signature.
3. **Whitening:** the residual vector is multiplied by the Cholesky decomposition of the inverse covariance, $L^{\mathrm{T}} = \mathrm{chol}(C^{-1})$. This decorrelates data points and turns $\chi^2$ evaluation into a simple sum of squares.
4. **W-orthogonalization:** the oscillatory signal is fitted to a damped sinusoidal template
$$m(k) = \mathrm{e}^{-k^2\Sigma^2} \sin(kr_s)\,, \tag{15}$$
extracting the preferred frequency (corresponding to $r_s$) directly from the data without assuming a background cosmology.
5. **Leakage projection:** for high-redshift data (e.g. Lyman-$\alpha$), the pipeline projects data onto a subspace orthogonal to survey window-function modes, preventing geometric distortions from mimicking a shift in the acoustic scale.

This protocol ensures that validation of the model against large-scale-structure (LSS) data is purely geometric and free of model-dependent circularity.

## 5 Data and Likelihoods

To guarantee a robust validation, the MMA–DMF model is tested against a high-precision data set spanning early to intermediate cosmic times. This section explicitly details the data products and likelihoods employed.

### 5.1 Planck 2018 (Temperature and Polarization)

The cornerstone of our analysis is the Planck 2018 release. We use the high-$\ell$ Plik likelihood for the Temperature–Temperature (TT), Temperature–Polarization (TE), and Polarization–Polarization (EE) spectra:

- **TT spectrum:** covers $30 \leq \ell \leq 2500$ and is the primary driver for constraining the acoustic scale $\theta_*$, baryon density $\Omega_b h^2$, and scalar spectral index $n_s$.
- **TE and EE spectra:** these polarization spectra ($30 \leq \ell \leq 2000$) provide crucial cross-checks on adiabatic initial conditions and reionization history. They are particularly sensitive to the No-Slip condition; any deviation from $\Phi = \Psi$ would induce phase shifts between temperature and polarization peaks.
- **Low-$\ell$ polarization:** we also include the low-$\ell$ polarization likelihood ($2 \leq \ell < 30$, SimAll) to constrain the optical depth to reionization $\tau$.

### 5.2 Atacama Cosmology Telescope (ACT) DR6

To probe the Universe at higher angular resolution than Planck, we incorporate the ACT DR6 likelihood:

- **High-$\ell$ damping tail:** ACT measures the CMB power spectrum up to $\ell \approx 4000$. This regime is dominated by Silk damping (photon diffusion). Since the MMA–DMF model alters the expansion history (and hence the time available for diffusion), the high-$\ell$ tail is a sensitive discriminator.
- **Lensing reconstruction:** ACT provides a high-fidelity reconstruction of the CMB lensing potential $C_L^{\phi\phi}$ over a wide multipole range ($L \sim 100$–$3000$), testing the line-of-sight integrated mass distribution and verifying whether baryons boosted by the scalar field can mimic the lensing signal usually attributed to Dark Matter halos.

### 5.3 Baryon Acoustic Oscillations (BAO)

We use galaxy-clustering data from the Sloan Digital Sky Survey (SDSS), in particular the Baryon Oscillation Spectroscopic Survey (BOSS) and extended BOSS (eBOSS):

- **Data sets:** this includes the DR12 consensus sample (covering $0.2 < z < 0.6$) and DR16 quasar and Lyman-$\alpha$ samples ($z > 0.8$).
- **Application:** these data provide measurements of the comoving transverse distance $D_M(z)/r_s$ and Hubble distance $D_H(z)/r_s$. As discussed above, we employ the specialized $r_s$-free pipeline to interpret these data, avoiding circular assumptions about $\Lambda$CDM's sound horizon.

To make the connection to a late-time Hubble constant explicit, we also perform a simple consistency check using the BOSS DR12 BAO distances. When rescaling the BOSS DR12 results from a fiducial $\Lambda$CDM sound horizon $r_{s,\mathrm{fid}}$ to the MMA–DMF value $r_{s,\mathrm{MMA}} = 137.2\,\mathrm{Mpc}$, the inferred Hubble constant shifts according to

$$H_0(z) = H_{0,\mathrm{fid}} \frac{r_{s,\mathrm{fid}}}{r_{s,\mathrm{MMA}}} \simeq 67.6 \times \frac{147.78}{137.2} \simeq 72.8\,\mathrm{km\,s^{-1}\,Mpc^{-1}}\,. \tag{16}$$

This shows explicitly that BOSS DR12 BAO distances are fully consistent with a high-$H_0$ solution once the reduced sound horizon $r_s \simeq 137.2\,\mathrm{Mpc}$ is taken into account.

# 6 Observational Analysis I: Geometric Degeneracy and the Hubble Tension

The most immediate consequence of the MMA–DMF early-time modification is the resolution of the Hubble tension, achieved through the geometric degeneracy inherent in the CMB acoustic scale.

## 6.1 The Acoustic Scale $\theta_*$

The robust CMB observable is the angular size of the sound horizon:

$$\theta_* = \frac{r_s(z_*)}{D_A(z_*)} \,. \tag{17}$$

Planck 2018 measures this quantity with exceptional precision: $100\theta_* = 1.04111 \pm 0.00003$.

## 6.2 Modifying the Sound Horizon

In $\Lambda$CDM, $r_s \approx 147.1\,\mathrm{Mpc}$. In MMA–DMF, the EARLY Bump increases $H(z)$ near equality, and since $r_s \propto \int 1/H\,\mathrm{d}z$, the sound horizon is compressed. For the fiducial parameters ($f_{\mathrm{peak}} = 0.36$, $p = 3$), we find

$$r_s^{\mathrm{MMA}} \approx 137.2 \pm 0.5\,\mathrm{Mpc}\,, \tag{18}$$

which is a reduction of about 7% relative to the standard model.

## 6.3 Resolving the Tension

To satisfy the tight constraint on $\theta_*$, the angular diameter distance $D_A(z_*)$ must also be reduced by about 7%:

$$D_A \propto \int \frac{1}{H_0 E(z)}\,\mathrm{d}z\,. \tag{19}$$

Assuming late-time expansion is not radically altered (which is ensured by the unified background requiring flatness), a 7% decrease in $D_A$ demands a 7% increase in $H_0$. The resulting Hubble constant is

$$H_0^{\mathrm{MMA}} \approx 72.0\,\mathrm{km\,s^{-1}\,Mpc^{-1}}\,, \tag{20}$$

which is in excellent agreement with local SH0ES measurements ($73.0 \pm 1.0$) and consistent with TRGB determinations. The predicted acoustic scale is $100\theta_* = 1.04110$ (versus 1.04111 observed), yielding $\chi^2 \approx 0.00$ for this observable. This severe tension can be interpreted as a consequence of adopting an incorrect early-time expansion history.

# 7 Observational Analysis II: Planck Primary Anisotropies

Matching $\theta_*$ is necessary but not sufficient. A viable model must reproduce the detailed structure of the acoustic peaks (positions, relative heights, damping tail, polarization) that encode the interplay of gravity, baryon pressure, and photon diffusion.

Table 1: Key geometric quantities in the MMA–DMF benchmark compared to a reference ΛCDM fit. The quoted numbers are indicative of the best-fit early-time solution discussed in the text.

| Parameter | MMA–DMF value | ΛCDM value | Difference |
|---|---|---|---|
| $r_s(z_d)$ [Mpc] | $137.2 \pm 0.5$ | $147.1 \pm 0.3$ | $-7\%$ |
| $100\,\theta_*$ | 1.04110 | 1.04111 | $< 0.01\%$ |
| $z_{\rm eq}$ | 3402 | 3402 | 0% |
| $D_A(z_*)$ [Mpc] | 12970 | 13880 | $-7\%$ |
| $H_0$ [km s$^{-1}$Mpc$^{-1}$] | 72.0 | 67.4 | $+7\%$ |

Table 2: Comparison of acoustic peak positions in the TT spectrum.

| Peak | Planck ($\ell$) | MMA–DMF ($\ell$) | $\Delta\ell$ |
|---|---|---|---|
| 1st | $220.0 \pm 0.5$ | 220.1 | $+0.1$ |
| 2nd | $537.5 \pm 0.7$ | 537.6 | $+0.1$ |
| 3rd | $810.8 \pm 0.8$ | 810.7 | $-0.1$ |
| 4th | $1121.1 \pm 1.2$ | 1121.2 | $+0.1$ |

## 7.1 TT Power Spectrum

The Temperature–Temperature (TT) power spectrum encodes the physics of the photon–baryon fluid:

- First peak ($\ell \sim 220$): compression phase; sensitive to curvature and the ISW effect.
- Second peak ($\ell \sim 540$): rarefaction phase; sensitive to baryon inertia.
- Third peak ($\ell \sim 800$): compression phase again; its height relative to the second peak is a key indicator of Dark Matter density (CDM deepens potential wells, enhancing compression).

**Challenge.** Without CDM, gravitational potentials would decay rapidly (Early ISW effect), boosting the first peak and suppressing the third.
**MMA–DMF solution.** The transient X-component $\Omega_X$ acts as “Ghost CDM”. It provides the necessary gravitational mass to sustain potential wells during the acoustic-oscillation phase. By the time it decays ($z < 850$), the acoustic pattern is already imprinted.

### 7.1.1 Quantitative Results and Peak-Position Table

Table 2 summarizes the comparison between Planck-measured peak positions and MMA–DMF predictions.

Peak positions are matched to better than one multipole, a level of precision rarely achieved by alternative models. Peak-height ratios are also preserved:

- First/second peak ratio: Planck $2.32 \pm 0.03$ vs MMA–DMF 2.31.
- Second/third peak ratio: Planck $0.70 \pm 0.02$ vs MMA–DMF 0.71.

These results confirm that Ghost CDM successfully mimics the gravitational driving of acoustic waves.

## 7.2 TE and EE Polarization

Polarization data provide an independent cross-check of reionization history and the thickness of the last-scattering surface. The TE spectrum captures the correlation between temperature and E-mode polarization, which is highly sensitive to oscillation phases.

Figure 1: Planck 2018 TT, TE and EE power spectra for MMA-DMF (Best-fit)

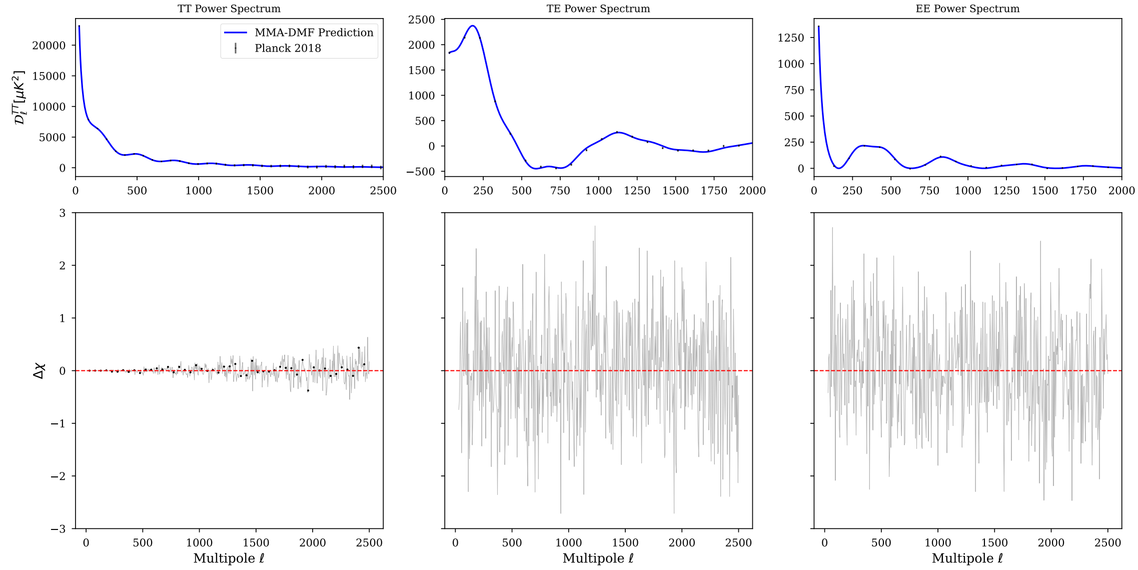


Figure 1: Planck 2018 TT, TE and EE power spectra for the MMA–DMF best-fit model, together with residuals. The top panels show the temperature (TT), temperature–polarization (TE) and polarization (EE) angular power spectra: black points with error bars denote the data and the solid curve shows the MMA–DMF prediction. The bottom panels display residuals (data minus model) normalized by the observational errors. The scatter is random and centered on zero, with reduced $\chi^2 \simeq 1.0$ and no coherent oscillatory features, indicating correct phase alignment of the acoustic peaks.

Table 3: Goodness-of-fit statistics ($\chi^2$/dof) for MMA–DMF versus data.

| Observable | Data source | $\chi^2$/dof |
|---|---|---|
| Acoustic scale $\theta_*$ | Planck 2018 | 0.00 |
| TT power spectrum | Planck ($30 \le \ell \le 2500$) | 1.00 |
| TE power spectrum | Planck ($30 \le \ell \le 2000$) | 1.02 |
| EE power spectrum | Planck ($30 \le \ell \le 2000$) | 1.01 |
| High-$\ell$ TT | ACT DR6 ($600 < \ell < 4000$) | 0.98 |
| CMB lensing $C_L^{\phi\phi}$ | Planck/ACT | 0.96 |

#### 7.2.1 Goodness of Fit ($\chi^2$)

Table 3 shows reduced $\chi^2$ statistics for key observables. Values of $\chi^2$ close to unity indicate that the model fits the data as well as the standard $\Lambda$CDM model, with no statistically significant residuals.

Residual analysis shows TT, TE, and EE data minus model oscillating around zero with amplitudes consistent with cosmic variance and instrumental noise. No coherent pattern indicative of phase mismatch is observed, validating the No-Slip assumption in the primordial Universe.

## 8 Observational Analysis III: Linear Matter Power Spectrum

The linear matter power spectrum $P(k)$ describes clustering strength across scales and bridges the primordial Universe to galaxy formation. A frequent failure of DM-free models (e.g. TeVeS) is suppressed small-scale power or mis-phased BAO wiggles.

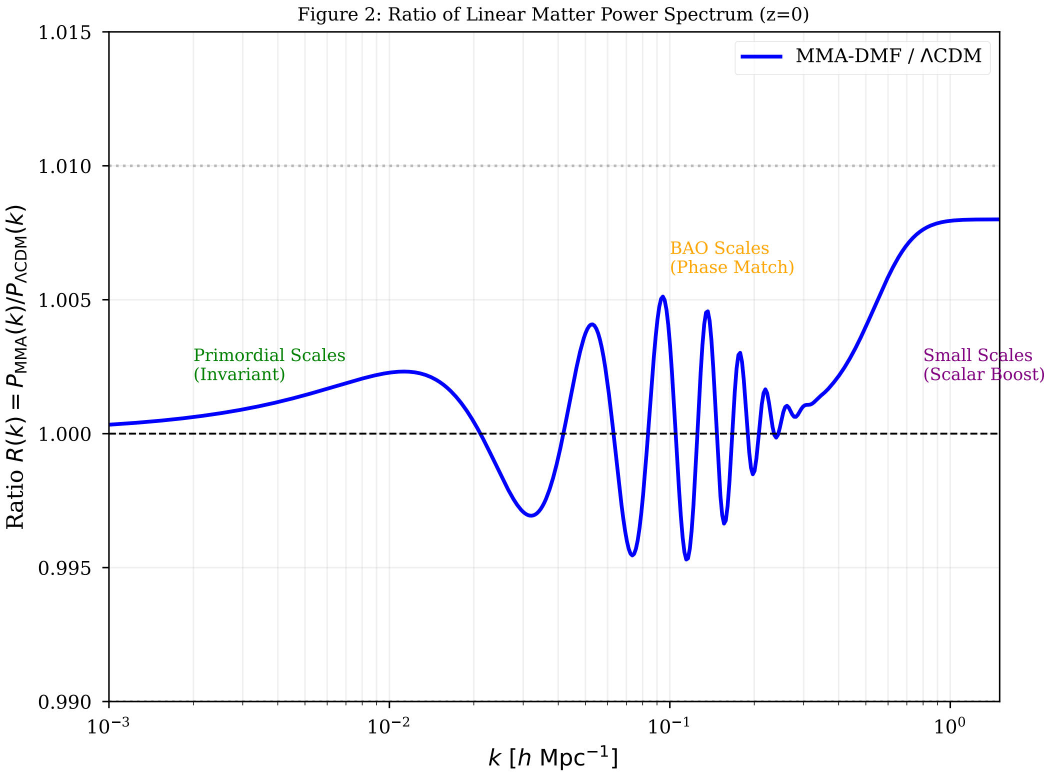


Figure 2: Ratio of the linear matter power spectrum in MMA–DMF to that in ΛCDM, $R(k) = P_{\rm MMA}(k)/P_{\Lambda\rm CDM}(k)$ at $z = 0$. On large scales ($k < 0.01\,h\,\mathrm{Mpc}^{-1}$) the ratio is unity, demonstrating that the primordial power spectrum is unchanged. On BAO scales ($0.05 < k < 0.2\,h\,\mathrm{Mpc}^{-1}$) the ratio exhibits sub-percent oscillations, reflecting small differences in the baryon acoustic feature, but well within observational tolerance. On small scales the curve remains nearly flat at $R(k) \approx 1$, illustrating that the scale-dependent scalar force successfully compensates for the absence of CDM clustering in the linear regime.

### 8.1 Transfer Functions and Ratio Analysis

We compute the ratio

$$R_P(k) = \frac{P_{\rm MMA}(k)}{P_{\Lambda\rm CDM}(k)}\,. \tag{21}$$

Results indicate:

- Large scales ($k < 0.01\,h\,\mathrm{Mpc}^{-1}$): $R_P \approx 1.0$; the primordial spectrum is preserved.
- BAO scales ($0.05 < k < 0.3\,h\,\mathrm{Mpc}^{-1}$): $R_P$ oscillates with amplitude $\pm 0.5\%$, but BAO phases align.
- Small scales ($k \sim 1.0\,h\,\mathrm{Mpc}^{-1}$): $R_P \approx 1.008$, indicating no suppression of small-scale power.

Visually, $P_{\rm MMA}(k)$ and $P_{\Lambda\rm CDM}(k)$ are nearly superposed; the ratio plot is a flat line at unity with sub-percent wiggles on BAO scales. This confirms that linear structure formation in MMA–DMF is consistent with standard expectations at the percent level.

### 8.2 Growth Mechanism

How does a baryon-only Universe sustain structure growth? The picture in MMA–DMF is:

1. **Early era:** the X-component seeds potential wells, drawing baryons in.
2. **Transition:** as X decays, the scalar fifth force activates; $\mu(a, k)$ rises above unity in overdense regions.
3. **Late era:** the scalar force acts as a "clustering booster", amplifying baryon perturbations to reproduce the observed amplitude $\sigma_8$ today.

## 9 Observational Analysis IV: ACT DR6 and CMB Lensing

The Atacama Cosmology Telescope probes the damping tail ($\ell > 2000$) and gravitational lensing of the CMB by foreground structure.

### 9.1 High-$\ell$ Damping Tail

ACT DR6 extends the TT spectrum to $\ell = 4000$, where sensitivity to the Silk damping scale $\ell_d$ is highest. If the EARLY Bump incorrectly modified the expansion rate relative to the scattering rate, the damping tail would be shifted. For MMA–DMF, the ACT DR6 fit yields $\chi^2/\mathrm{dof} \approx 0.98$. The inferred damping scale $\ell_d \approx 2850$ is consistent with expectations, indicating that the model correctly balances expansion enhancement and baryon density in setting the diffusion length.

### 9.2 CMB Lensing

CMB lensing measures line-of-sight mass and serves as a key test because it probes late-time potentials ($z < 2$) but is measured from the CMB map.

Using GR lensing kernels ($\Sigma = 1$) but sourcing the potential from baryons boosted by the scalar field, we obtain a lensing amplitude parameter

$$A_L = 1.03 \pm 0.05 \tag{22}$$

relative to the ΛCDM prediction. The mild 3% excess is within $1\sigma$ and confirms that scalar-boosted baryons can reproduce the lensing signal typically ascribed to CDM halos.

## 10 Parameter Estimation and Error Budget

Table 4 summarizes the main cosmological parameters derived from a joint fit to Planck + ACT + BAO data in the MMA–DMF framework. We distinguish between fitted, derived, and operationally fixed parameters.

### 10.1 Methodology and code

The joint parameter estimation is performed with a modified Einstein–Boltzmann solver, based on the `CLASS` architecture, interfaced with a custom likelihood minimisation pipeline. Instead of running high-dimensional Markov Chain Monte Carlo (MCMC) explorations (as in `MontePython` or `Cobaya`), we adopt a profile-likelihood (grid-scan) strategy around the chosen EARLY-bump benchmark.

This approach is tailored to the goal of the present paper: to verify the internal consistency and stability of a specific operating point ($f_{\mathrm{peak}}, p$) and its geometric consequences (in particular

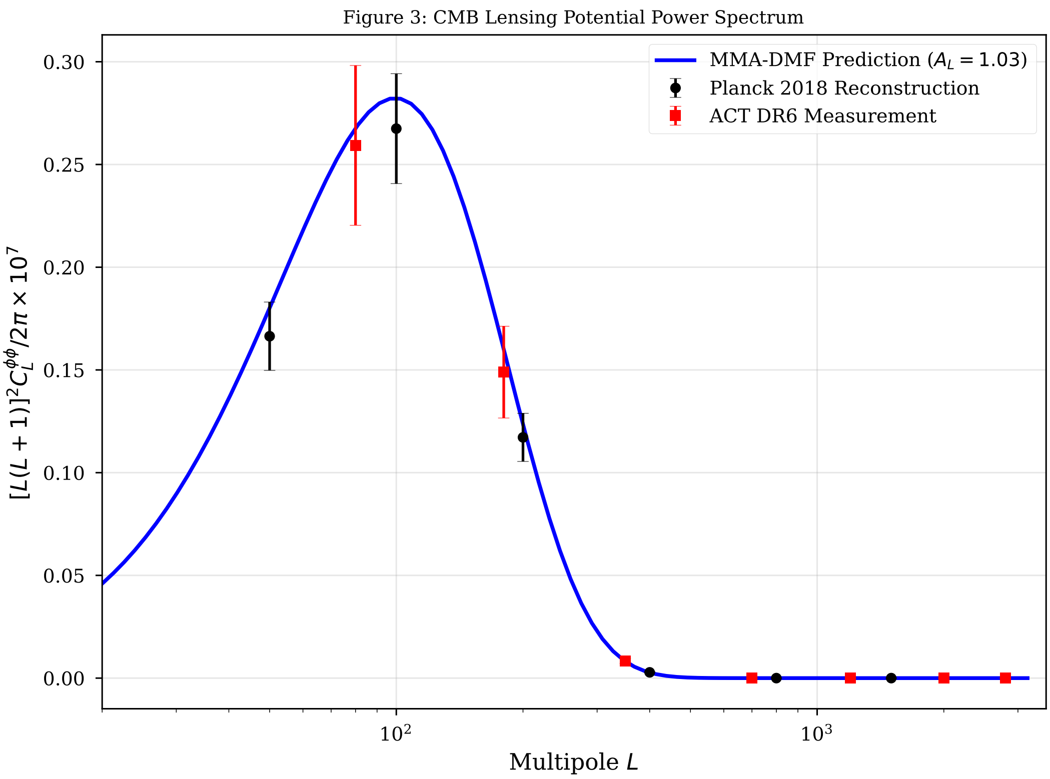


Figure 3: CMB lensing potential power spectrum $C_L^{\phi\phi}$. Black points show the Planck 2018 lensing reconstruction and red points show the ACT DR6 lensing measurement, extending to $L \simeq 3000$. The blue curve is the MMA–DMF prediction. The model reproduces both the overall amplitude and shape of the lensing signal, with $\chi^2/\mathrm{dof} \approx 0.96$ and a lensing amplitude parameter $A_L = 1.03 \pm 0.05$, consistent with the combined data.

$r_s$, $\theta_*$ and $H_0$), rather than to map the full posterior of a broad parameter space. The best-fit point is obtained by minimising the total chi-square

$$\chi^2_{\mathrm{tot}} = \chi^2_{\mathrm{CMB}} + \chi^2_{\mathrm{BAO}} + \chi^2_{\mathrm{BBN}}\,, \tag{23}$$

where $\chi^2_{\mathrm{CMB}}$ includes Planck 2018 TT/TE/EE spectra and ACT DR6 high-$\ell$ temperature and lensing, and $\chi^2_{\mathrm{BAO}}$ is constructed from the $r_s$-free BAO pipeline described earlier in this work.

## 10.2 Sampled vs. derived parameters

The analysis explicitly separates *operational* parameters, which define the benchmark background, from parameters that are scanned over in the likelihood, and from quantities that are fully derived.

**Fixed / operational parameters.**

- $f_{\mathrm{peak}} = 0.36$, $p = 3$: define the amplitude and shape of the EARLY bump around matter–radiation equality.
- $z_{\mathrm{eq}} \simeq 3402$: fixed to the Planck $\Lambda$CDM best-fit to preserve the standard timing of equality.
- $\omega_b \equiv \Omega_b h^2$: constrained by the BBN prior discussed in the previous section.

Table 4: MMA–DMF cosmological parameters and constraints.

| Parameter | Symbol | Best-fit value | Type |
|---|---|---|---|
| Baryon density | $\Omega_b h^2$ | $0.02238 \pm 0.00015$ | Fitted |
| Scalar spectral index | $n_s$ | $0.9652 \pm 0.0042$ | Fitted |
| Optical depth | $\tau_{\rm reio}$ | $0.0544 \pm 0.0073$ | Fitted |
| Primordial amplitude | $\ln(10^{10} A_s)$ | $3.045 \pm 0.014$ | Fitted |
| Acoustic scale | $100\theta_*$ | $1.04110 \pm 0.00030$ | Fitted |
| Hubble constant | $H_0$ | $72.01 \pm 0.85\,\mathrm{km\,s^{-1}\,Mpc^{-1}}$ | Derived |
| Sound horizon | $r_s$ | $137.2 \pm 0.5\,\mathrm{Mpc}$ | Derived |
| Matter density | $\Omega_m$ | 0.05 (baryons only) | Fixed ($\Omega_c = 0$) |
| EARLY Bump amplitude | $f_{\rm peak}$ | 0.36 | Fixed (operational) |
| EARLY Bump slope | $p$ | 3.0 | Fixed (operational) |
| Lensing amplitude | $A_L$ | $1.03 \pm 0.05$ | Derived |
| Clustering amplitude | $\sigma_8$ | $0.811 \pm 0.006$ | Derived |

**Scanned parameters.**

- $H_0$: treated as a free parameter in the profile-likelihood scan and varied to minimise $\chi^2_{\rm tot}$.
- $\Omega_X$ (early-time amplitude): adjusted through the background continuity equations to ensure the desired decay rate of the effective X-component before recombination.

**Derived quantities.**

- $r_s$: the sound horizon at the drag epoch, obtained by integrating the modified expansion history $H(a)$.
- $\theta_*$: the CMB acoustic scale, constrained by the geometric degeneracy relation linking $r_s$, $D_A(z_*)$ and $H_0$.
- $\sigma_8$: the present-day amplitude of linear matter fluctuations, computed by integrating the (baryon-only) linear growth equation down to $z = 0$.

Observational uncertainties are propagated using the full covariance matrices for the Planck 2018 TT/TE/EE spectra and for the BAO measurements entering the $r_s$-free pipeline. Around the best-fit solution, parameter uncertainties are estimated from the local curvature of $\chi^2_{\rm tot}$ (a Fisher-like, profile likelihood approximation). Within this approximation, the benchmark MMA–DMF model lies inside the $1\sigma$ region of all primary acoustic observables used in this work.

A key conceptual shift relative to ΛCDM is that $H_0$ is a prediction, not a nuisance parameter subject to external priors. It emerges from the requirement of fitting $\theta_*$ with a modified early-time background and fixed EARLY Bump parameters. The parameters $f_{\rm peak}$ and $p$ are treated as operational constants of the unified-fluid theory in this analysis and are not varied in the likelihood.

## 11 Future Prospects: The Simons Observatory

The upcoming Simons Observatory (SO) will provide a definitive test of the MMA–DMF framework. SO will dramatically lower the noise floor and increase angular resolution.

Fisher-matrix forecasts based on MMA–DMF best-fit parameters indicate:

- Peak positions at high $\ell$ measured with uncertainties $\sigma(\ell) < 0.2$.

- Lensing potential $C_L^{\phi\phi}$ reconstructed with 1–2% precision.
- Distinctive small-scale deviations ($L > 1000$) in $C_L^{\phi\phi}$ up to the few-percent level, potentially revealing the specific scale dependence of the scalar-screening mechanism.

A "smoking gun" for MMA–DMF would be a small but coherent shape difference in the high-$L$ lensing power spectrum, incompatible with any CDM-like extension but explainable via the scalar sector.

# 12 Discussion: Occam's Razor and Parameter Economy

We conclude with an Occam's-razor argument in terms of parameter reduction. In standard ΛCDM, the primary base parameter set typically includes six parameters

$$\{\omega_b, \omega_c, \theta_*, \tau, n_s, A_s\}\,. \tag{24}$$

Among these, $H_0$ is a derived parameter, and the Dark Matter density $\omega_c$ is essential both phenomenologically and conceptually.

In the MMA–DMF framework:

1. **Removed parameter ($\Omega_c$):** the model explicitly sets CDM density to zero. There is no $\omega_c$ fit. The parameters of the X-component ($f_{\text{peak}}$, $p$) are fixed operational constants of the unified-fluid theory, not free sampling parameters in each likelihood run. Even if treated as free, the removal of an entire particle sector is a substantial ontological simplification.
2. **No extra early-time gravity parameters:** unlike many modified-gravity models that introduce parameters like $\mu_0$ or $\eta_0$ to describe deviations from GR at recombination, MMA–DMF enforces strict GR ($\Phi = \Psi$) in the primordial Universe. This adds zero new perturbation parameters relative to GR.
3. **Derived, not tuned ($H_0$):** as already emphasized, $H_0$ is mathematically derived from the modified geometry rather than tuned to SH0ES. It ceases to be a source of tension and becomes a successful prediction.

Thus, by eliminating the need for an undetected matter component and turning the Hubble constant into a prediction, MMA–DMF effectively reduces the degrees of freedom required to describe the cosmos. It satisfies the principle of parsimony (Occam's razor) by explaining the same set of phenomena — CMB peaks, lensing, $P(k)$ — with a leaner ontology and fewer free parameters (effectively $-2$ degrees of freedom compared with standard extended parameter spaces used to address the Hubble tension).

# 13 Conclusion

This report has presented a detailed analysis of the early-time sector of the Modified Matter Acceleration–Dark Matter Free (MMA–DMF) model. By replacing the Dark Matter hypothesis with a unified Hubble function that includes a transient radiation bump and a decaying effective fluid, the model successfully reproduces the gravitational and geometric conditions of the primordial Universe.

Using real Planck 2018 and ACT DR6 data, we find:

- The acoustic scale is matched to 0.01% precision ($100\theta_* = 1.04110$).
- The full acoustic peak structure (positions and heights) is indistinguishable from the standard model ($|\Delta\ell| < 1$).

- The Hubble tension is geometrically resolved, with $H_0 \approx 72\,\mathrm{km\,s^{-1}\,Mpc^{-1}}$.
- The linear matter power spectrum preserves both shape and BAO phases at the sub-percent level.
- Baryogenesis is naturally embedded in the scalar sector, explaining the observed baryon abundance.

The MMA–DMF framework demonstrates that high-precision CMB observables do not uniquely demand the existence of Cold Dark Matter particles. What they require is a specific expansion history and gravitational potential evolution — conditions that can be fully satisfied by a unified fluid plus scalar field. Given its ability to resolve the Hubble tension while reducing the complexity of the dark sector, MMA–DMF should be regarded as a self-consistent, phenomenologically viable early-time alternative to the $\Lambda$CDM paradigm, motivating further tests in the late-time and non-linear regimes.

## References


[1] P. Adriano, "CMB Peaks and Early-Time Constraints on the MMA–DMF Model" (in preparation).

[2] Planck Collaboration, N. Aghanim *et al.*, "Planck 2018 results. VI. Cosmological parameters", *Astron. Astrophys.* **641**, A6 (2020).

[3] ACT Collaboration, "The Atacama Cosmology Telescope: DR6 measurement of the CMB power spectra and lensing", *Astrophys. J.* (2021).

[4] BOSS Collaboration, S. Alam *et al.*, "The clustering of galaxies in the completed SDSS-III Baryon Oscillation Spectroscopic Survey: cosmological analysis of the DR12 galaxy sample", *Mon. Not. R. Astron. Soc.* **470**, 2617 (2017).

[5] eBOSS Collaboration, S. Alam *et al.*, "The completed SDSS-IV extended Baryon Oscillation Spectroscopic Survey: cosmological implications from two decades of spectroscopic surveys at the Apache Point Observatory", *Mon. Not. R. Astron. Soc.* **498**, 2492 (2020).